

PVP2011-57051

**ANALYSIS OF ABWR CONTAINMENT PRESSURE-TEMPERATURE LOADS AND SUPPRESSION POOL HYDRODYNAMICS FOLLOWING LOSS OF COOLANT ACCIDENTS**

**P. Sawant**  
 Energy Research, Inc.  
 P.O. Box 2034  
 Rockville, Maryland 20843 USA

**M. Khatib-Rahbar**  
 Energy Research, Inc.  
 P.O. Box 2034  
 Rockville, Maryland 20843 USA

**F. Moody**  
 2125 N. Olive Ave., D-33  
 Turlock, California 95382 USA

**A. Drozd**  
 United States Nuclear Regulatory Commission  
 Washington, D.C. 20555 USA

**ABSTRACT**

This paper focuses on the assessment of Advanced Boiling Water Reactor (ABWR) containment pressure-temperature and suppression pool hydrodynamics under design-basis, loss-of-coolant accident (LOCA) conditions. The paper presents a phenomena identification and ranking table (PIRT) applicable to the ABWR containment response behavior, modeling of pressure-temperature loads using the MELCOR computer code, and analysis of suppression pool hydrodynamics parameters based on a mechanistic one-dimensional hydrodynamics model. A MELCOR 1.8.6 model with detailed nodalization of the ABWR containment is used to perform the containment pressure-temperature calculations following a design basis accident. The best estimate and several sensitivity calculations are performed for the ABWR containment using the suppression pool swell model. The sensitivity calculations demonstrate the influence of key model parameters and assumptions on the suppression pool hydrodynamics response. The comparison of containment pressure-temperature and the suppression pool swell analyses results to those reported in the ABWR licensing calculations showed reasonable agreement.

**INTRODUCTION**

The ABWR, is a 3,926 MW(t) reactor housed in a pressure suppression containment that includes a drywell and a wetwell/suppression pool compartment. Figure 1 illustrates the overall layout of the ABWR primary containment (ABWR DCD, 1997). Any pressure build-up inside the drywell exceeding the vent submergence pressure differential will result in vent clearing and passage of gases through the water pool

into the wetwell gas space. For as long as the suppression pool remains subcooled, any steam vented in this manner would be expected to substantially condense. Wetwell-to-drywell vacuum breakers are also present to permit gas flow and pressure equalization if wetwell pressure was ever to exceed the drywell pressure.

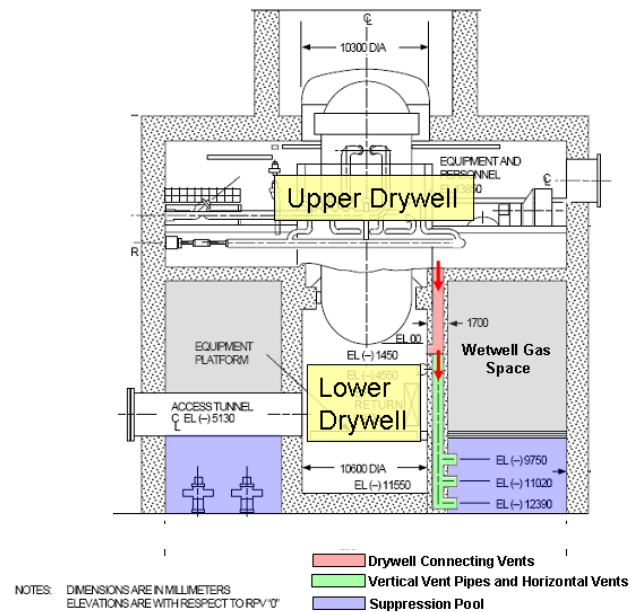


Fig. 1 ABWR containment (ABWR DCD, 1997)

Design basis analyses for ABWR containment involve estimation of maximum pressures and temperatures inside the drywell and wetwell following loss-of-coolant accidents (LOCAs); a feed water line break (FWLB) and a main steam line break (MSLB) inside the containment. In addition to this, assessment of hydrodynamic loads that are generated due to the rapid swelling of suppression pool on the wetwell internal structures (e.g., the safety relief valve (SRV) discharge piping, catwalk structure, wetwell-to-drywell vacuum breaker etc.) is also an essential part of the ABWR containment design analyses. The pressurization of drywell during the initial phase of LOCA results in suppression pool vent clearing and rapid flow of drywell gases (primarily nitrogen) through the suppression pool into the wetwell gas space. The flow of drywell gases through the drywell to wetwell vents creates large, expanding bubbles at the horizontal vent exits. These bubbles expand against the suppression pool hydrostatic and the gas space pressures, as the air/steam mixture flow continues from the pressurized drywell. As a result, the water ligaments (or liquid slugs) on top of the expanding bubbles accelerate upward, which give rise to the pool swell phenomena that typically last 2 to 3 seconds. The rising pool surface can impact and impose loads on structures that are located inside the wetwell. To predict the pool swell hydrodynamic loads on these wetwell internal structures, it is essential to determine various pool swell parameters such as the maximum pool surface elevation, peak pool surface velocity, peak wetwell gas space pressure, and peak bubble pressure (before the bubble breakthrough).

The containment analysis methodology developed by General Electric (GE) for MARK III containment (Bilanin, 1974) was used to perform the pressure-temperature analysis presented in the ABWR design control document (DCD) (ABWR DCD, 1997). Furthermore, the suppression pool swell analysis presented in the ABWR DCD was performed using the GE proprietary computer code PICSIM. This code was validated against the MARK III Pressure Suppression Test Facility (PSTF) data. The Final Safety Analysis Report (FSAR) (South Texas Project [STP] Units 3 and 4 FSAR, 2010) submitted to the United States Nuclear Regulatory Commission (NRC) in support of the combined license (COL) application utilized the Generation of Thermal-Hydraulic Information for Containments (GOTHIC) computer code for the containment pressure-temperature and pool swell analyses. The GOTHIC-approach has also been benchmarked against the MARK III PSTF data (STP Units 3 and 4 FSAR, 2007).

The objective of this paper is to present the results of the independent analyses of the ABWR containment. The pressure-temperature analysis was performed using the MELCOR computer code. A mechanistic model developed by Sawant and Khatib-Rahbar (2011) for prediction of various suppression pool hydrodynamic parameters (i.e., vent clearance, pool surface elevation, pool surface velocity, wetwell gas space and the bubble pressure) is utilized for the pool swell analysis. A comparison of the current results against the GOTHIC

pressure-temperature and pool swell analyses results (STP Units 3 and 4 FSAR, 2010) is presented. The paper also examines the sensitivity of containment pressure-temperature and pool swell parameters to major assumptions and governing model parameters. A brief discussion on the PIRT, which is used as a basis for assessing the applicability of MELCOR and for the development of the pool swell analysis model, is also presented in this paper. Finally, the paper also presents the results of comparison of the suppression pool swell model to the BWR MARK III PSTF experimental data.

## **DOMINANT PHENOMENA**

Annex A shows the PIRT applicable to ABWR containment pressure-temperature and suppression pool swell response during the design basis accidents (i.e., FWLB and MSLB). The importance rankings assigned in the PIRT were delineated based on the expected impact of the phenomenon on maximum containment pressure-temperature and pool swell parameters (i.e., maximum pool surface elevation, peak pool surface velocity, peak wetwell gas space pressure, and peak bubble pressure). Separate ranking is assigned for the short- and long-term response of containment pressure-temperature (the importance ranking for long-term is shown in the bracket only if it is different compared the short-term ranking). The dominant phenomena that are modeled to analyze suppression pool hydrodynamics in the pool swell model (Sawant and Khatib-Rahbar, 2010) are highlighted in the PIRT. A brief description of some of the important phenomena identified in the PIRT is provided in this section.

The phenomena identified in the PIRT can be broadly classified into following categories:

- (a) Mass and energy release to containment;
- (b) Drywell atmosphere mixing and heat transfer;
- (c) Vent clearance and flow through vertical and horizontal vents;
- (d) Formation, growth, rise, and breakthrough of bubble in suppression pool; and
- (e) Suppression pool mixing and heat transfer.

The drywell pressurization rate is a function of the rate of mass and energy release into the drywell from the reactor pressure vessel (RPV) and the piping sides of the break. The break flow from the piping side of the break primarily consists of stored inventory of coolant inside the piping. The break flow from the RPV side is determined by the RPV thermodynamic conditions. Several phenomena are identified in the PIRT that affect the RPV thermodynamic conditions and hence, the break flow rate. However, for the containment pressure-temperature analysis presented in this paper, the mass and energy release to containment are prescribed as input conditions. Furthermore, the transient drywell pressure and temperature are specified as boundary conditions to the suppression pool swell model. Consequently, the mass and energy release rate to drywell are not considered in this paper.

The drywell pressurization rate is also affected by many phenomena occurring inside the drywell including mixing in the drywell atmosphere, heat transfer to the drywell heat structures, and transport of liquid droplets in the drywell atmosphere. Mixing of the vapor and liquid droplets discharged from the break and the drywell non-condensable gases (mostly nitrogen, N<sub>2</sub>) determines the drywell thermodynamic conditions (pressure-temperature). It also affects the fraction of total drywell non-condensable gas transferred to the wetwell and determines the composition of flow entering the drywell connecting vents. Since this phenomenon directly influences the drywell pressure and temperature, it has been assigned high ranking. Usually for conservative analysis, the assumption of complete mixing of the non-condensable gases, vapor, and droplets is made (ABWR DCD, 1997). The homogeneous drywell mixture assumption results in the utmost transfer of the drywell non-condensable gases to the wetwell gas space.

The fraction of break flow entering in the form of droplets affects the drywell thermodynamic conditions. Depending on the initial velocity and size, the droplets have different residence time in the drywell atmosphere. The smaller droplets stay in the drywell atmosphere for a longer time before settling on to the drywell structures (walls or floors) compared to the larger droplets. Since the smaller droplets have higher surface to volume ratio and longer residence time, the interfacial heat transfer between these droplets and drywell atmosphere can significantly affect the drywell thermodynamic conditions.

Heat transfer to the drywell structures (e.g., containment wall.) includes forced or natural convection from the drywell atmosphere, condensation of steam on the structural surfaces, and by deposition or precipitation of droplets on structural surfaces. This phenomenon is ranked low for the short-term period analysis considering the fact that the ABWR containment is inerted with nitrogen gas. Since the transfer of energy to the heat structures in the drywell would effectively decrease the containment pressure and temperature, it is usually neglected for a conservative analysis (ABWR DCD, 1997).

Predicting the vent clearance time and flow through the vents (drywell connecting vents, vertical vent pipe, and horizontal vents) is essential for modeling the containment pressure-temperature response and the pool swell phenomena. The vent clearance time is the time required for the transfer of water from the drywell-to-wetwell vent system to the suppression pool after a LOCA. It determines the time required for the initiation of a pool swell following a LOCA. Furthermore, the flow of the drywell gases through the vents following the vent clearance affects the drywell pressure, the bubble growth rate, and the magnitude of the pool swell parameters. The processes affecting the vent clearance time include the inertia of water inside the vent system and the pool, the hydrostatic head of water inside the pool, the friction and form losses in the vent system (including the flow regimes), and the back pressure at the exit of the horizontal vents (due to the expanding bubble and the inertia of the liquid slug after the clearance of the top vents).

The flow rate of the drywell gas mixture through the vents following the vent clearance is mainly affected by various pressure losses through the vent system, including the losses due to fluid inertia, spatial acceleration, gravity, friction, and form losses (due to wall friction, contraction/expansion, and bends). Higher pressure losses through the vent system result in higher drywell pressure, lower vent flow rate, and a relatively less severe pool swell response. Therefore, for the pressure-temperature analysis, the assumption of a maximum pressure loss is bounding and for the pool swell analysis, the assumption of a minimum pressure loss is bounding.

A peak containment pressure is determined by the amount of non-condensable gases transferred from the drywell to the wetwell airspace. Since the lower drywell volume is approximately 25% of the total drywell volume, it is important to determine the amount of non-condensable gas that can be transferred from the lower drywell to the wetwell. It has been noted in the ABWR DCD (1997) that due to peculiar design of the lower drywell and the drywell connecting vents connecting the upper drywell to the lower drywell, transfer of non-condensable gases from the lower drywell to wetwell is possible only after the peak drywell pressure is reached. Therefore, this phenomenon has been assigned low ranking for the short-term response. However, it is necessary to perform sensitivity calculations to study the effect of gas trapping inside the lower drywell.

Following the clearance of horizontal vents, the drywell contents are purged into the suppression pool. This leads to the transfer of energy from the drywell non-condensable gases, vapors and liquid to the suppression pool. Most of the vapors condense in the suppression pool and the non-condensable gases accumulate in the wetwell gas space. The important phenomena in the suppression pool includes direct contact condensation of vapors in the presence of non-condensable gases, mixing of the pool and thermal stratification, transfer of energy to the suppression pool heat structures, and bubble dynamics and its effect on pool swell height and velocity. Since during the blowdown period, prior to the activation of the Residual Heat Removal (RHR) system, the suppression pool is the ultimate sink for the energy released from the RPV into the containment, an accurate prediction of condensation heat transfer rate in presence of non-condensable gases is essential for the estimation of suppression pool temperature and wetwell and drywell pressures. Therefore, this phenomenon has been assigned high ranking for short- and long-term analysis.

Predicting the growth rate of the bubble that is formed at the exit of horizontal vent is important because it determines the magnitude of various pool swell parameters. This phenomenon is not important to the pressure-temperature analysis. The bubble growth rate is governed by the difference in the pressures inside and outside the bubble. In the present pool swell model, the growth rate of the bubble is calculated from the solution (Sawant and Khatib-Rahbar, 2010) to the Raleigh equation (Carey, 2007). The phenomena/parameters affecting the inside pressure of the bubble include the vent

mass flow rate and the interfacial heat and mass transfer at the bubble and suppression pool water interface. The interfacial heat and mass transfer at the interface of the bubble is due to the steam (which is part of the drywell gas mixture) at this interface and the cooling of the non-condensable gases in the bubble resulting from the transfer of heat to the suppression pool water. If either the drywell gas mixture or the vent gas flow discharge includes some percentage of steam, the growth rate of the bubble will be lower. The higher growth rate is obtained by assuming that 100 percent of the atmosphere in the drywell is only occupied by nitrogen. Furthermore, the interfacial heat transfer between the gas bubble and the suppression pool affects both the gas temperature and the growth rate of the bubble. During a LOCA, the drywell air temperature is usually higher than the suppression pool temperature. The reduction in the temperature of the gas in the bubble due to the interfacial heat transfer to the suppression pool water will effectively reduce the growth rate of the bubble. An assumption of 100 percent nitrogen in the drywell and the absence of the interfacial heat and mass transfer would result in a higher growth rate of the bubble and more bounding predictions for various pool swell parameters.

The outside pressure of the bubble is affected by the hydrostatic head and inertia of the liquid slug over the bubble. Additionally, the compression of the wetwell gas space due to a rising suppression pool surface also influences this outside pressure. Pressurization of the wetwell gas space reduces the growth rate of the bubble. Isothermal compression would result in a lower wetwell gas space pressure and a higher bubble growth rate (hence, a higher pool swell height and pool surface velocity). On the other hand, adiabatic compression would result in a higher wetwell gas space pressure and a lower bubble growth rate.

The bubble rise velocity and bubble breakthrough time determine the termination of the pool swell transient. The bubble rises through the suppression pool due to the combined effects of buoyancy and drag forces acting on the bubble. These forces are functions of the size and shape of the bubble. As the size increases, the buoyancy force on the bubble increases and the shape of the bubble also changes. The bubbles formed during the pool swell transient are relatively large in size (due to the large horizontal vent diameter of 70 cm). They do not exactly match any of the well-known bubble types for which bubble rise velocity measurements are available (see Figs. 11-12 of Lahey, Jr. and Moody, 1993). Judgment is needed to predict the rise velocity of growing bubbles that are being charged from the horizontal vents. Furthermore, the rise velocity of a slug bubble is affected by the presence (or absence) of wetwell gas space pressurization.

## **PRESSURE-TEMPERATURE ANALYSIS**

### **Applicability of MELCOR**

The applicability of MELCOR for the ABWR containment pressure-temperature analysis is assessed by considering the

adequacy of MELCOR for modeling the high ranked phenomena identified in the PIRT. As noted earlier, for the current analysis, the mass and energy release to containment are prescribed as boundary conditions. Therefore, phenomena related to the mass and energy release rate to drywell (i.e. break flow and enthalpy) are not considered in the MELCOR applicability assessment presented in this section.

Mixing of gases and droplets in drywell atmosphere can be simulated in MELCOR by representing the drywell volume with the multiple control volumes connected by several flow paths. However, as noted earlier, the homogeneous drywell mixture assumption results in the utmost transfer of the drywell non-condensable gases to the wetwell gas space. Therefore, in the current analysis, the whole drywell volume (including the lower drywell) is represented by a single control volume. As shown later by a sensitivity analysis, this assumption results in higher containment pressurization.

In MELCOR, the size of droplets and their deposition rate can be controlled using the parametric models. A parametric flashing model allow the user to specify the droplet size distribution for the liquid fraction of the break flow that is being injected into the drywell. The deposition of fog (droplets) can be controlled in MELCOR by specifying a maximum fog density parameter (default is 0.1 kg/m<sup>3</sup>).

The heat transfer to the drywell heat structures is modeled using the heat structure package in MELCOR. However, for the current analysis, the heat losses to drywell heat structures are neglected for the short-term pressure-temperature analysis.

The vent clearance time and flow through the vents can be modeled in MELCOR by representing the vent system using the control volume and flow path packages. As noted earlier, the clearance time is mainly influenced by the inertia of water inside the vertical vent and hydrostatic head in suppression pool. MELCOR is capable of modeling the hydrostatic pressure drop. In order to model the inertia effect in MELCOR, it is necessary to prescribe the inertia lengths for the flow paths representing the horizontal vents. Furthermore, the gas flow rate through the vents following the vent clearance is mainly affected by friction and form losses. In MELCOR, the form loss coefficient for a flow path is specified as user input. Due to uncertainty involved in estimation of form loss coefficients, a sensitivity calculation is performed to investigate the influence of the effective vent loss coefficient on the calculated drywell pressure and temperature.

In MELCOR, condensation is calculated using a bubble physics model which is activated for the horizontal vent flow paths. The model uses a parametric approach involving estimation of two efficiency coefficients for the determination of condensation rate of vapors in the gas bubbles. Default values for the model parameters implies that the condensation efficiency is 1.0 if the pool subcooling is more than 5 K and the pool depth is 1.0 cm above the flow path opening height. For the ABWR containment, initial suppression pool subcooling is 40 K and the submergence depth of the top horizontal vents is

more than 3 m. Therefore, complete condensation of vapors in suppression pool is calculated by the MELCOR model.

Effects of pool mixing and thermal stratification can be modeled in MELCOR by dividing the suppression pool into several control volumes and by manipulating the interconnecting flow paths; however, as shown in the PIRT, thermal stratification is not expected to be of any significance inside the ABWR suppression pool under the design basis accident conditions. Therefore, the representation of the suppression pool using a single control volume is sufficient for the current analysis.

MELCOR cannot model the bubble dynamics and its effects on suppression pool swell height velocity. However, simulation of these phenomena is not essential for the containment pressure-temperature analysis. These phenomena are considered in the suppression pool swell analysis model.

It is concluded that the MELCOR is capable of modeling the high ranked phenomena that are identified in the PIRT for application to the pressure-temperature response analysis.

### MELCOR Model

A MELCOR 1.8.6 model was developed for the ABWR containment. The model consists of separate control volumes for the Drywell (DW), Drywell Connection Vents (DCVs), Vertical Vent Pipes, and Wetwell (see Fig. 2). The upper drywell and lower drywell control volumes are combined to create a single drywell control volume. The flow paths 211, 212, and 213 connecting the vertical vent pipes to the suppression pool represent the top, middle and bottom rows of the horizontal vents, respectively. The influence of the inertia of water inside the vertical vent pipes, the horizontal vents, and the suppression pool on vent clearance is accounted by specifying the effective inertia lengths for the horizontal vent flow paths. Vertical flow paths connecting the drywell connecting vent and the vertical vent pipe control volumes (FL206, 207, & 208) are designed to account for the form losses in drywell connecting vents, vertical vent pipe, and horizontal vents. At a given time, depending on water level inside the vertical vent, only one flow path (FL206, 207, or 208) is active. This modeling approach enables representation of the variable vent form loss, which depends on the number of horizontal vents open.

### Initial and Boundary Conditions

Initial conditions for the containment are obtained from STP Units 3 and 4 FSAR (2010). Following the approach used in ABWR DCD (1997) and STP Units 3 and 4 FSAR (2010), the entire lower drywell volume is assumed to be perfectly mixed with the upper drywell volume during the MSLB case, but only half of the lower drywell volume is assumed to mix with the upper drywell for the FWLB event. The MELCOR calculations begin with a simulation of normal, pre-accident steady-state conditions of duration 50 seconds.

The break mass and energy releases provided in the STP Units 3 and 4 FSAR (2010) for the FWLB and MSLB

accidents are applied as boundary conditions to the MELCOR model. Figures 3 and 4 show mass and energy released to containment in FWLB accident scenario. FWLB is a double-ended rupture in one of the two main feedwater lines inside the containment. The break mass flow rate and energy from the feedwater system side (or balance of plant side) of the break are shown in Fig. 3. Similarly, the break mass and energy flow rates from the RPV side of the break are shown in Fig. 4.

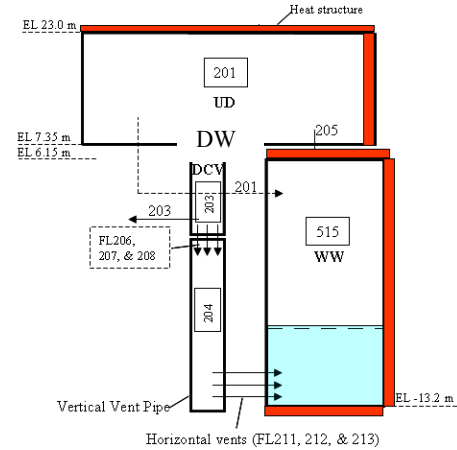


Fig. 2 MELCOR containment nodalization

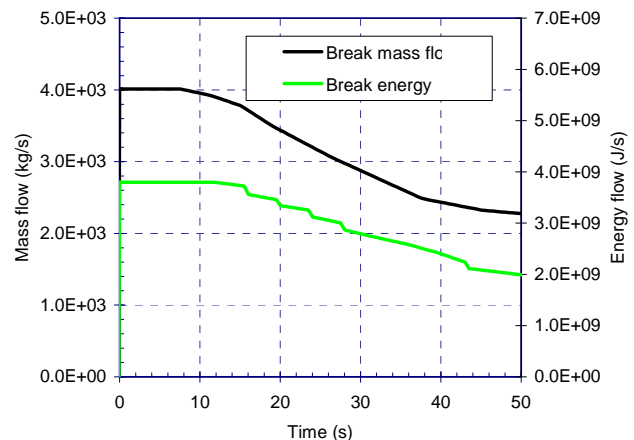


Fig. 3 Break mass and energy flows from feed-water system side of the break in FWLB LOCA

### Pressure-Temperature Analysis Results

The short- and long-term simulations of FWLB and MSLB accidents are performed using the MELCOR containment model. The results for the base and sensitivity case calculations are discussed in this section. The model assumptions for the base case simulations are very similar to the GOTHIC model assumptions as documented in the STP Units 3 and 4 FSAR (2010) (e.g., single drywell node, homogeneous mixing in drywell, etc.). The sensitivity calculations studied the impact of drywell nodalization (single vs. two drywell nodes), effective vent loss coefficient, and drywell node volume (only for FWLB simulation). The sensitivity calculations are performed only for the short-term simulations. Only the results for the short-term FWLB base and sensitivity case calculations are discussed in

detail below. The summary of FWLB and MSLB base case analyses is presented in Table 1.

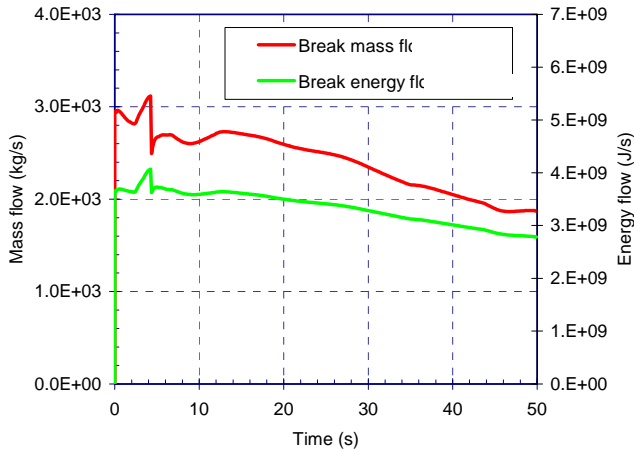


Fig. 4 Break mass and energy release rates from RPV side of the break during FWLB LOCA

Figure 5 shows the comparison of MELCOR- and GOTHIC-calculated drywell and wetwell pressures in the short-term FWLB simulation. Similar comparison for the drywell temperature is shown in Fig. 6. Figure 6 also shows the MELCOR-calculated wetwell temperature (GOTHIC-calculated wetwell temperature is not available). As observed from these figures, the MELCOR predictions are in close agreement with the GOTHIC results. Similar conclusions can be drawn from the comparison of suppression pool temperatures predicted by GOTHIC and MELCOR (not shown here). During this simulation, all three horizontal vents open within 1.3 to 2.3 s and remain open thereafter (i.e., 50 s). The molar gas compositions of the drywell and suppression pool gas space shows that within the first 30 s following the accident, most of the nitrogen in the drywell is replaced by the steam and transferred to the wetwell gas space.

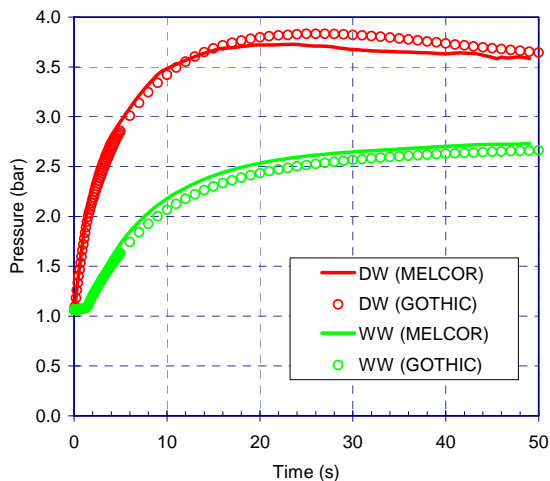


Fig. 5 Comparison of MELCOR- and GOTHIC-calculated containment pressures in FWLB LOCA

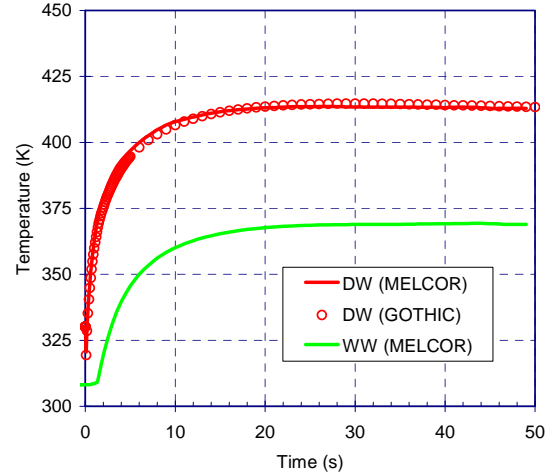


Fig. 6 Comparison of MELCOR- and GOTHIC-calculated containment temperatures in FWLB LOCA

Figure 7 shows the comparison of MELCOR base case and sensitivity case drywell pressures for the short-term FWLB simulation. The peak drywell pressures predicted in the two drywell node and reduced vent loss coefficient sensitivity cases are lower than the base case simulation. Consideration of full lower drywell volume gives higher drywell peak pressure as compared to the base-case. The two drywell node sensitivity calculation is performed to demonstrate the impact of dividing the drywell control volume into two separate lumped nodes (i.e., the upper and the lower drywell compartments). The use of two drywell nodes results in relatively less amount of non-condensable gases to transfer from drywell to the wetwell gas space (or more gases are entrapped in the lower drywell volume). Consequently the peak drywell pressure predicted in this sensitivity case is lower than the base-case simulation using one drywell node.

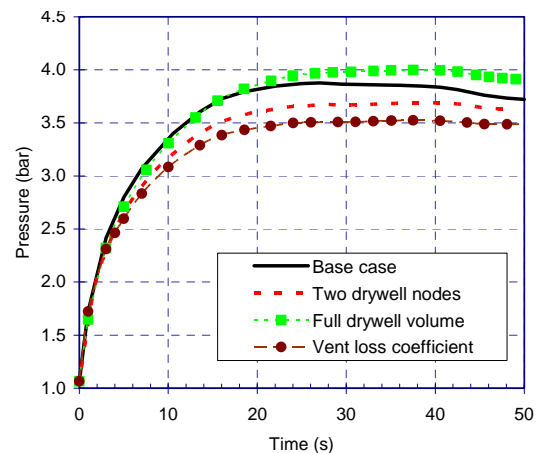


Fig. 7 Sensitivity of containment pressure

The total volume of the drywell node in the base case FWLB simulation is defined as 50% of the free volume of the lower drywell plus 100% of the free volume of the upper

drywell. To test the sensitivity of drywell pressure and temperature to this assumption, the sensitivity calculation credits the full volume of the drywell, i.e., 7190.65 m<sup>3</sup>. As shown in Fig. 7, the consideration of full drywell volume results in significant increase of peak drywell and wetwell pressures. Even though the total volume of the drywell is higher for the sensitivity calculation, the total amount of non-condensable gases transported to the wetwell gas space is also higher (due to additional mass of nitrogen corresponding to the 50% of the lower drywell free volume). This leads to relatively higher compression of wetwell gas space and higher wetwell pressurization.

In the vent loss coefficient sensitivity calculation, the effective vent loss coefficient is set to unity under all conditions. As noted earlier, depending on the number of cleared horizontal vent rows, a different value is used for this loss coefficient. The base-case calculation uses higher effective vent loss coefficients. As shown in Fig. 7, reduction of the effective vent loss coefficient results in a significant reduction of the peak drywell pressure. Lower pressure losses in the vent system result in faster transfer of drywell gases to the wetwell; and thereby, lower drywell pressurization rate. Consequently, the peak drywell pressure predicted in the sensitivity case is lower than the base-case simulation.

Table 1 shows the comparison of maximum values estimated for the drywell pressure, drywell temperature, wetwell pressure, wetwell gas space temperature, and suppression pool temperature in the STP Units 3 and 4 FSAR (2010) using GOTHIC and the present base case MELCOR analyses (includes short- and long-term FWLB and MSLB simulations). The table also shows the ABWR containment design limits for these parameters. As observed from this table, the MELCOR-estimated maximum values for drywell temperature and suppression pool liquid temperature are lower than the GOTHIC predictions. MELCOR predicts higher maximum values for drywell pressure, wetwell pressure, and wetwell gas space temperature; however, these predictions show that the maximum loads remain below the design limits. As observed from the table, the GOTHIC results show a safety margin of about 10% for the drywell pressure, which is similar when compared to the safety margin of 8% as predicted by the present MELCOR calculations. The GOTHIC-calculated maximum drywell temperature (short-term MSLB) exceeds the drywell design temperature of by 2°C for about 2 seconds. However, due to thermal inertia, the drywell structures (in particular the upper head seals) would not be expected to reach the design temperature limit during this short time frame.

### SUPPRESSION-POOL HYDRODYNAMICS

A simple one-dimensional analytical model based on fundamental physical principles was developed by Sawant and Khatib-Rahbar (2011) for the prediction of suppression pool swell parameters. The PIRT documented in Annex A identifies the dominant phenomena that are represented in this model. Detailed derivation of the model is available in Sawant and

Khatib-Rahbar (2011). A brief description of the model is given below.

Table 1 Comparison of MELCOR and GOTHIC results

Design Parameter	Design Limit*	GOTHIC	MELCOR
Drywell pressure, kPaG	309.9	281.8	287
Drywell temperature, K	444.4	446.4	440
Wetwell pressure, kPaG	309.9	210.3	236
Wetwell gas space temperature, K	377.2	371.8	373
Suppression pool temperature, K	373.2	372.7	370

\* Design limits as specified in STP Units 3 and 4 FSAR (2010)

### Suppression Pool Swell Model

The mathematical model for suppression pool swell analysis consists of equations modeling the vent clearance, the vent flow rate and pressured drop, the bubble growth rate (of bubbles which are formed at the horizontal vent exit), the bubble rise velocity and breakthrough time, the suppression pool surface velocity, and the wetwell gas space compression. Drywell pressure and temperature are supplied as boundary conditions to the model.

The vent clearance equation is derived by integrating a one-dimensional momentum equation from the surface of water inside the vertical vent pipe to the suppression pool surface. Several assumptions are considered in the derivation of this equation including the assumptions of the negligible pool surface velocity, the constant wetwell gas space pressure, and negligible pressure losses in the suppression pool (e.g., pool inertia). A sensitivity study shows that the vent clearance time is mainly influenced by the pressure losses due to inertia of water inside the vertical vent and hydrostatic head (Sawant and Khatib-Rahbar, 2011). The vent clearance equation calculates the water level inside the vertical vent. Based on this level, the vent clearance time (for top, middle, and bottom horizontal vents), gas and liquid phase effective vent system form loss coefficients (calculated by considering the geometry of vent system), and total effective horizontal vent flow area available for the gas and liquid flows are estimated.

As soon as the water level inside the vertical vent pipe drops below the top elevation of the top horizontal vent, the pool swell calculations are initiated. It involves estimation of vent pressure drop (for gas flow), bubble growth rate and rise velocity, pool surface velocity and elevation, and compression of gas space inside the suppression pool. The vent pressure drop equation is obtained by integrating one-dimensional momentum equation from the entrance of the drywell connecting vents to the exit of the horizontal vents. All horizontal vents (top, middle, and bottom) are assumed to be represented by a single horizontal vent located at the elevation of the top horizontal vent. Only frictional pressure loss is

considered in the vent pressure drop equation. The pressure drops due to inertia, spatial acceleration and gravity are neglected. Total effective horizontal vent flow area available for the gas flow and the gas phase effective vent loss coefficient used in the vent pressure drop equation are calculated (by considering the geometry of vent system) based on the water level inside the vertical vent.

A growth rate of a bubble, which is formed at the exit of horizontal vent, is governed by the bubble inside and outside pressures. The bubble growth rate is calculated using the Raleigh equation (Carey, 2007). The bubble inside pressure which is assumed to be same as the pressure at the exit of horizontal vent is obtained using the vent pressure drop equation. The bubble outside pressure is obtained by accounting for the inertia and hydrostatic head of a liquid slug on the top of the bubble and pressurization of wetwell gas space. Once the bubble growth rate and size are known, the pool surface velocity and elevation can be estimated using simple correlations. The bubble rise velocity is estimated empirically (by assuming cap or slug bubble shapes) to determine the bubble breakthrough elevation and time. The calculation is terminated immediately after the bubble breakthrough occurs. The feedback effects of the pool level swell phenomena on vent clearance phenomena are not considered in this model. The pressurization of the wetwell gas space volume due to pressure suppression pool surface rise is calculated by assuming the polytropic compression of an ideal gas.

The model has been benchmarked against the BWR Mark III containment PSTF experimental data (Sawant and Khatib-Rahbar, 2011). Three PSTF experiments were selected for the comparison. The selected experiments used air as the blowdown fluid. The results of comparison show that the predicted vent clearance time for the top vent, pool swell height, and the bubble breakthrough elevation are within 10 percent of the experimental data. The liquid slug thickness and the pool surface velocity are predicted within 30% of the experimental data.

### **ABWR Containment Pool Swell Analysis**

The suppression pool swell model described above is used to analyze the pressure suppression pool hydrodynamics in the ABWR containment. The analyses include best estimate and sensitivity calculations. The sensitivity calculations are performed to study the impact of key model assumptions on the pool swell parameters. Furthermore, the model predictions are also compared with comparable results based on GOTHIC calculations, as documented in the STP Units 3 and 4 FSAR (2010). The drywell pressure and temperature boundary conditions used in the current analyses are derived from the STP Units 3 and 4 FSAR (2010), which provides pressure and temperature transient data in the drywell and wetwell for the design-basis feedwater and main steam line break accidents.

Best estimate (base case) and sensitivity calculations were performed for the ABWR containment to assess the impact of

various model inputs on the calculations of various pool swell parameters. The model input parameters/assumptions that were selected for the sensitivity calculations include (a) the pressure suppression pool surface area, (b) the polytropic constant for wetwell gas compression, and (c) the effective vent form loss coefficient. The best estimate values of these parameters were used for the base case calculations. In order to account for the non-uniform pool swell, only 80% suppression pool surface area was considered in the ABWR DCD (1997) and STP Units 3 and 4 FSAR (2010) pool swell analyses. The best estimate (or base case) simulations that are presented in the current study use the 100 percent value of the pool surface area. However, similar to the ABWR DCD (1997) and the STP Units 3 and 4 FSAR (2010) pool swell analyses, in order to account for the effect of the non-uniform pool swell within the present one-dimensional modeling framework, the results of a sensitivity calculation that also assumes an 80 percent value for the pool surface area are presented.

The polytropic gas constant ( $\gamma$ ) used in wetwell gas space compression equation affects the wetwell gas space compression.  $\gamma=1.4$  is equivalent to assuming an adiabatic compression (for nitrogen gas) and  $\gamma=1.0$  is equivalent to assuming an isothermal compression. The adiabatic compression assumption results in a relatively higher wetwell gas space pressure and a lower pool swell and pool surface velocity (due to a higher wetwell gas space pressure). The assumption of isothermal compression results in a relatively higher suppression pool swell and pool surface velocity and a lower wetwell gas space pressure. The time duration of the pool swell phenomena is about 2 to 3 seconds. Consequently, the transfer of heat between the wetwell gas space and the wetwell heat structures are not significant. Therefore, for the best estimate (base case) analysis, the adiabatic compression  $\gamma=1.4$  is assumed.

The best estimate values of the effective gas flow vent form loss coefficient are calculated using the approach presented in Sawant and Khatib-Rahbar (2010). The calculated effective vent form loss coefficient varies from 4.3 to 14.9 depending on the number of horizontal vents that are open. These values are used for the base case calculation. For the sensitivity case calculation, a negligibly small (around 0.1) form loss is assumed under all vent flow configurations.

Table 2 shows the results of the best estimate (base case) and sensitivity case pool swell calculations and the values of the sensitivity parameters used in each calculation. For each calculation, the table also shows the predicted bubble breakthrough time, maximum pool swell height, maximum pool surface velocity, maximum bubble pressure, and maximum wetwell gas space pressure.

The sensitivity case calculation with an 80 percent pool surface area shows a substantial increase in the maximum pool surface velocity and pool swell height. The maximum pool surface velocity is increased by 25 percent and the maximum pool swell rise height is increased by 53 percent compared to

the predictions for the base case. The results of sensitivity case calculation with the isothermal compression of the wetwell gas space show only small increase in the maximum pool surface velocity (4.5 percent). Furthermore, the maximum wetwell gas space and bubble pressures are reduced (-3 to -5 percent) when compared to the base case results. The most significant effect on the all pool swell parameters is observed in a sensitivity case with an effective vent form loss coefficient value of 0.1. Table 2 shows that the maximum pool swell is increases by 106 percent in this sensitivity calculation. Similarly, the maximum pool surface velocity increases by 58 percent; and the maximum wetwell gas space and bubble pressures increase by more than 20 percent.

Table 2 Best estimate and sensitivity case calculation results

Parameters	Base Case	Sensitivity Cases		
		1	2	3
Pool surface area, %	100.0	<b>80.0</b>	100.0	100.0
Polytropic constant	1.4	1.4	<b>1.0</b>	1.4
Vet loss coefficient	Top	14.9	14.9	<b>0.1</b>
	Top & middle	5.9	5.9	<b>0.1</b>
	All	4.3	4.3	<b>0.1</b>
Breakthrough time, s	1.66	1.75	1.66	1.78
Maximum pool swell, m	1.5	2.3	1.5	3.1
Maximum pool surface velocity, m/s	4.3	5.4	4.5	6.8
Maximum bubble pressure, kPa	153	158	148	184
Maximum wetwell gas space pressure, kPa	129	134	122	163

### Comparison to Licensing Analyses

The STP Units 3 and 4 FSAR (2010) pool swell analysis for the ABWR containment was performed using the GOTHIC code. Table 3 shows the comparison of peak values estimated for the pool swell height, pool surface velocity, wetwell gas space pressure, and bubble pressure in the STP Units 3 and 4 FSAR (2010) GOTHIC analysis and those based on the present model. Generally, good agreement in the results is noted.

Table 3 Comparison with GOTHIC (2010) results

Pool Swell Parameter	GOTHIC (2010)	Present Model
Maximum pool swell height, m	8.8	8.7
Maximum pool surface velocity, m/s	10.9	9.5
Maximum WW gas pressure, kPaG	146	161
Maximum bubble pressure, kPaG	195	179

### CONCLUSIONS

The ABWR containment pressure-temperature analyses using the MELCOR code included several base case and sensitivity case simulations. The results of the base-case calculations simulating FWLB and MSLB accidents showed that the MELCOR predictions of the peak containment pressure

and temperature are in good agreement to those reported in the STP Units 3 and 4 FSAR (2010) using GOTHIC. The results of the sensitivity calculations showed that the assumptions of the single drywell node and higher vent loss coefficient are conservative for the ABWR containment pressure-temperature analysis. Accounting for a full lower drywell volume in the short-term FWLB simulation results in higher peak drywell pressure.

The PIRT-based highly ranked phenomena were represented mechanistically in the pool swell analysis model developed by Sawant and Khatib-Rahbar (2010). The base case and sensitivity case calculations were performed to assess the impact of key model assumptions on various pool swell parameters. The sensitivity calculations show that the assumption of a smaller pool surface area (to account for the uneven pool swell) and reduced vent loss coefficients are the most bounding in terms of their impact on the calculation of suppression pool swell parameters. Finally, the model was applied to conditions corresponding to a LOCA inside the ABWR containment. Comparisons of the calculated results to those reported in the STP Units 3 and 4 FSAR (2010) using GOTHIC showed reasonable agreement.

### ACKNOWLEDGMENTS

This work was performed under the auspices of the United States Nuclear Regulatory Commission, Office of New Reactors, Contract Number NRC-42-07-483.

### REFERENCES

1. ABWR DCD, 1997. ABWR Design Control Document Revision 4. <http://www.nrc.gov/reactors/new-reactors/design-cert/abwr.html>.
2. Bilanin, W.J., 1974. The General Electric Mark III Pressure Suppression Containment System Analytical Model, Licensing Topical Report, NEDO-20533.
3. Carey, V.P., 2007. Liquid-Vapor Phase-Change Phenomena, second ed. Hemisphere Publishing Corporation, New York.
4. Lahey, Jr., R.T., Moody, F.J., 1993. The Thermal-Hydraulics of a Boiling Water Reactor, Second Ed. American Nuclear Society, La Grange Park, Illinois.
5. Sawant, P. and Khatib-Rahbar, M., 2011. Modeling of Suppression Pool Hydrodynamics in the ABWR Containment, paper submitted for publication in Nuclear Engineering and Design (under review)
6. South Texas Project (STP) Units 3 and 4 FSAR, 2010. South Texas Project Units 3 and 4 COLA (FSAR) Revision 3. <http://adamswebsearch2.nrc.gov/idmws/ViewDocByAccession.asp?AccessionNumber=ML102860517>.
7. Wallis, G.B., 1969. One-Dimensional Two-Phase Flow. McGraw-Hill, New York.

## ANNEX A

### PHENOMENA IDENTIFICATION RANKING TABLE APPLICABLE TO ABWR CONTAINMENT UNDER DESIGN BASES ACCIDENT CONDITIONS

Phenomenon/Process	Importance Ranking	
	Pressure-Temperature*	Pool Swell
<b>Mass and Energy Release from RPV and Piping Side</b>		
Stored energy in vessel & core assemblies and heat transfer to coolant	L (M)	L
Decay heat to coolant (short- and long-term)	L (M)	L
Scram and core power during blowdown	L (M)	L
RPV two-phase level swell (core and downcomer) and two-phase and single-phase blowdown intervals	M (L)	L
Two-phase and single phase critical flow	H	H
Break flow flashing (generation of droplets and vapors)	H (L)	H
Initial pipe inventory and double ended blowdown interval	H (L)	H
<b>Drywell Atmosphere Mass and Energy Transfer</b>		
Mixing and transport of non-condensable gases and water vapor	H	H
Droplet transport (break-up, coalescence, evaporation, and droplet suspension or fallout)	H (M)	H
Heat transfer to drywell heat structures (steam condensation on surfaces) and wall heat transfer	L (M)	M
<b>Flow in Drywell Connecting Vents</b>		
Two-phase flow regime through drywell connecting vents	M	M
Flow losses in drywell connecting vents	M	M
<b>Lower Drywell Non-Condensable Gas Transport</b>		
Mixing and transport of non-condensable gases from lower drywell to wetwell gas space	L (M)	L
<b>Flow in Horizontal Vents</b>		
Vent clearance and fluid inertia	H (L)	M
Flow through vent (perfect gas, steam, gas-droplet mixture, and choked flow)	M (L)	M
Flow losses (bends, turns, geometric losses)	H (L)	H
Effect of back pressure and clearing time, sequential	M (L)	H
<b>Mass, Energy and Momentum Transfer in Suppression Pool</b>		
Direct contact condensation of vapors in suppression pool in presence of non-condensable gases	H	M
Suppression pool mixing and thermal stratification (Pool Heating)	L (M)	L
Gas bubble discharge	-	H
Pool swell and height	-	M
Bubble penetration	-	M
<b>Mass, Energy, and Momentum Transfer in Wet-well Gas Space</b>		
Gas sparging through the suppression pool	M	H
Wetwell pressurization	H (L)	H
Pool surface rise and compression of gas	L	H
Wetwell gas/vapor mixing and stratification	L	L
Heat transfer to wetwell heat structures	L (M)	L
Long term pool heating of gas	L (M)	L
<b>Suppression Pool Bypass Leakage</b>		
Flow of vapor mixture directly from drywell to wetwell gas space	L (M)	L

\* Rankings for long-term pressure-temperature response are shown in brackets (-)